Cell, Vol. 90, 717–727, August 22, 1997, Copyright ©1997 by Cell Press

Utrophin-Dystrophin-Deficient Mice as a Model for Duchenne Muscular Dystrophy

Anne E. Deconinck,*§# Jill A. Rafael,*#
Judith A. Skinner,* Susan C. Brown,†
Allyson C. Potter,* Laurent Metzinger,*
Diana J. Watt,‡ J. George Dickson,†
Jonathon M. Tinsley,* and Kay E. Davies*‖
*Genetics Unit
Department of Biochemistry
University of Oxford
South Parks Road
Oxford, OX1 3QU
United Kingdom
†School of Biological Sciences
Royal Holloway
University of London
Surrey, TW20 OEX
United Kingdom
‡Department of Anatomy
Charing Cross and Westminster Medical School
Fulham Palace Road
London W6 8RF
United Kingdom

Summary

The absence of dystrophin at the muscle membrane leads to Duchenne muscular dystrophy (DMD), a severe muscle-wasting disease that is inevitably fatal in early adulthood. In contrast, dystrophin-deficient *mdx* mice appear physically normal despite their underlying muscle pathology. We describe mice deficient for both dystrophin and the dystrophin-related protein utrophin. These mice show many signs typical of DMD in humans: they show severe progressive muscular dystrophy that results in premature death, they have ultrastructural neuromuscular and myotendinous junction abnormalities, and they aberrantly coexpress myosin heavy chain isoforms within a fiber. The data suggest that utrophin and dystrophin have complementing roles in normal functional or developmental pathways in muscle. Detailed study of these mice should provide novel insights into the pathogenesis of DMD and provide an improved model for rapid evaluation of gene therapy strategies.

Introduction

Duchenne muscular dystrophy (DMD) is a common (1/3300 boys), X-linked progressive muscle-wasting disease where patients are usually confined to a wheel chair in their early teens and die by their early twenties due to respiratory or cardiac failure (Emery, 1993). The disease is caused by lack of dystrophin, a large membrane-associated protein expressed in muscle and brain that is localized to the inner face of the cell membrane (for review, see Tinsley et al., 1994; Blake et al., 1996). The *mdx* mouse lacks dystrophin due to a mutation that results in a premature stop codon in exon 23 (Bulfield et al., 1984; Sicinski et al., 1989). Although this mouse has proved a valuable model for DMD, the progressive muscle-wasting disease presents itself in a much milder form than in humans, and the mice often live up to 2 years of age, which is comparable to the life span of wild-type mice (J. A. R., unpublished data). This difference might be attributable to the reduced life span of mice compared with humans, combined with a similar rate of progression of the disease. Alternatively, compensatory mechanisms present in mice may not have the same effects in humans, possibly due to an overall size difference and the overall force placed on the muscles.

mdx muscle appears histologically normal in the immediate postnatal period, but an acute phase of muscle necrosis occurs around weaning with visible muscle weakness (Cullen and Jaros, 1988). Many cellular and biochemical features resemble those characteristic of the early myopathic phase of DMD, such as elevated serum creatine kinase (CK) levels and accumulation of macrophages, which are indicative of muscle degeneration. *mdx* skeletal muscle then recovers by virtue of substantial muscle regeneration morphologically characterized by small-caliber centrally nucleated fibers, and *mdx* mice move and behave as normal mice. Upregulated levels of muscle transcription factors appear to be integral components of this successful regeneration. *mdx* mice lacking the muscle-specific transcription factor MyoD show a more severe dystrophy due to a deficiency in regenerative capabilities of the muscle (Megeney et al., 1996). The ability of the *mdx* mouse to compensate for lack of dystrophin by increasing regenerative activity is of interest not only in the investigation of dystrophin function and DMD pathology but also in the search for potential therapeutic agents.

Compensation for lack of dystrophin by structurally related proteins such as utrophin may also be more successful in the mouse, leading to a milder phenotype than in humans. Utrophin localizes at the sarcolemma of skeletal muscle fibers during fetal development; by birth, dystrophin replaces utrophin at the sarcolemma. Utrophin is now only present at neuromuscular and myotendinous junctions (NMJ and MTJ) (Bewick et al., 1992; Law et al., 1994). However, high levels of utrophin are present around the sarcolemma of regenerating myofibers in adult *mdx* skeletal muscle. Utrophin is also expressed in heart, brain, and in nonmuscle tissues that lack full-length dystrophin (Helliwell et al., 1992; Karpati et al., 1993; Pons et al., 1994a; Sewry et al., 1994). The high amino acid identity between utrophin and dystrophin in important functional domains suggests a possible redundancy between the two proteins. Both proteins feature an N-terminal domain that binds to F-actin in the cytoskeleton (Winder et al., 1995) and a

§Present address: Division of Hematology-Oncology, Childrens' Hospital, Howard Hughes Medical Institute, Harvard Medical School, Boston, Massachusetts 02115.
‖To whom correspondence should be addressed.
#The first two authors contributed equally to this work.

long rod domain of spectrin-like repeats. Utrophin also contains a high degree of similarity to the cysteine-rich and C-terminal regions of dystrophin that have been shown to interact with a set of transmembrane- and membrane-associated proteins known as the dystrophin-associated protein complex (DPC) (for review, see Ozawa et al., 1995). The DPC consists of α- and β-dystroglycan, α, β, γ, δ-sarcoglycan, and the syntrophins. β-dystroglycan has been shown to bind to the cysteine-rich region of dystrophin in vitro and has been proposed to be the direct link between dystrophin and the DPC (Ozawa et al., 1995). Dystrophin is thought to provide a link between the subsarcolemmal cytoskeleton and the extracellular matrix through this protein complex. Several autosomal recessive muscular dystrophies are caused by mutations in the genes encoding some of the DPC proteins (Campbell, 1995).

Recently, the expression of a utrophin minigene under the control of a human α-skeletal actin promoter in *mdx* mice has been shown to restore the DPC to the sarcolemma and to result in mice with greatly improved muscle pathology (Tinsley et al., 1996). These data suggest that the continued sarcolemmal presence of utrophin in skeletal muscle can lead to the functional replacement of dystrophin. However, these transgenic experiments do not indicate whether dystrophin and utrophin play complementary roles in normal muscle function and development. Recent reports of utrophin-null mutants indicate a structural role for utrophin in the formation or stabilization of junctional folds during NMJ maturation (Deconinck et al., 1997; Grady et al., 1997a). However, these mice do not display any overt phenotypic abnormalities or muscle weakness to date (12 months).

To investigate the interrelationship between utrophin and dystrophin in muscle, we interbred utrophin-null mice (*utrn*$^{-/-}$) with *mdx* mice. Double-knockout (dko) mice (*mdx/utrn*$^{-/-}$) show many more of the clinical signs of DMD than *mdx* mice, which show no phenotypic signs of their underlying muscle pathology and live a normal life span. Dko mice show an earlier age of onset of dystrophy in their diaphragm muscles, coexpression of myosin heavy chain (MHC) isoforms within skeletal muscle fibers, and a marked alteration in junctional folding at the neuromuscular and myotendinous junctions. The most obvious observation is that dko mice undergo weight loss after weaning with the onset of joint contractures and kyphosis, resulting in premature death

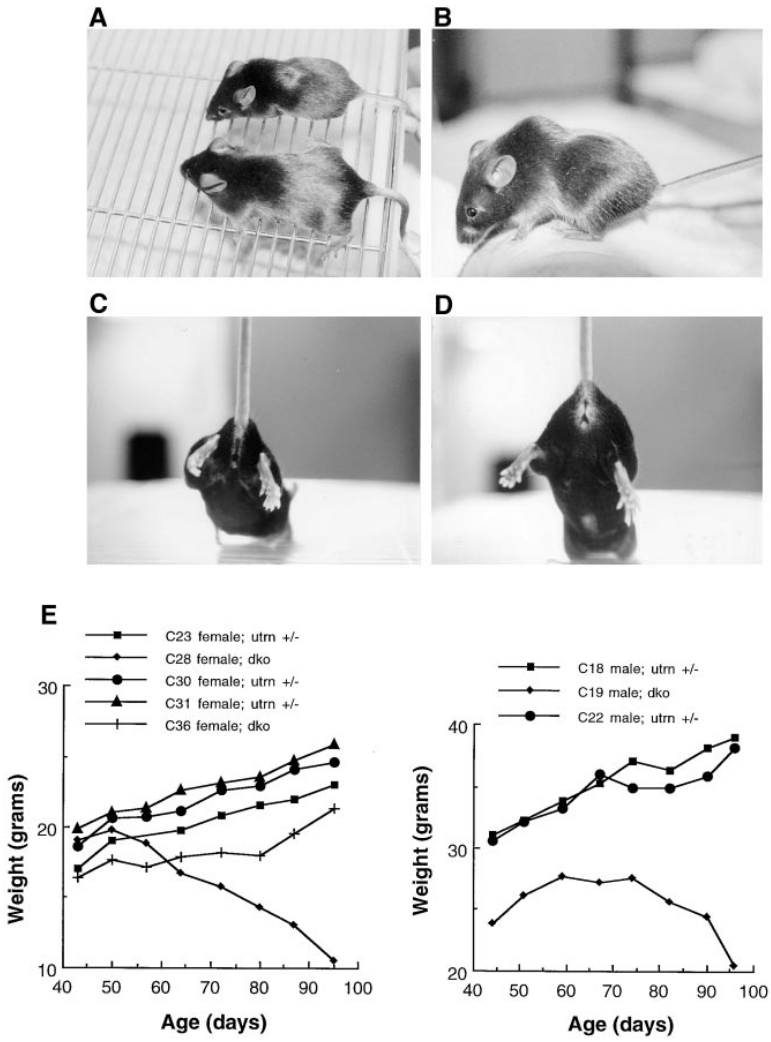

Figure 1. Utrophin/Dystrophin Deficiency Leads to DMD-like Pathological Signs

In contrast with *mdx* mice (A, bottom), which are physically indistinguishable from wild-type mice, dko mutants are smaller in size (A, top), with growth retardation starting around weaning and eventual weight loss (E). The mice are characterized by a slack posture (A), a progressive curvature of the spine (kyphosis, B), and an abnormal waddling gait. Their weight is carried on the hocks, which is presumably causing the waddling gait. The abnormal posture of the hind limbs and joint contractures are also evident when the mice are held by the tail (C) compared with normal mice that reach out their back legs (D).

by 20 weeks of age. These observations suggest that utrophin and dystrophin play synergistic roles in functional or developmental pathways in skeletal muscle. The testing of potential treatments for DMD in mice will require not only an assessment of the improvement of muscle pathology but an overall improvement in the clinical features of the disease. Such an assessment cannot be made in *mdx* mice, since their physical characteristics appear outwardly normal. The utrophin/dystrophin-deficient mice presented here may provide a more useful model for which to assess effective therapeutic strategies.

Results

Pathological Features of Mice Lacking Dystrophin and Utrophin

To study the function of the dystrophin and utrophin proteins and any redundancy between them, as well as the significance of utrophin upregulation in the *mdx* mouse, female *mdx* mice were mated to male utrophin knockout mice. The F1 offspring were further interbred following three different breeding schemes (described in Experimental Procedures). Dko mice were identified by ARMS assay PCR for dystrophin genotype (Amalfitano and Chamberlain, 1996) and Southern analysis or PCR for their utrophin genotype. The dko mutants were easily identifiable by 4 to 6 weeks of age by their slack posture and reduced weight (Figure 1A), lack of mobility, abnormal breathing pattern, and abnormal field behavior. These mice then showed progressive muscle weakness with marked kyphosis (profound, progressive dorsal-ventral curvature of the spine; Figure 1B), a characteristic waddling gait with weight bearing on abnormally postured hind limbs with joint contractures (Figure 1C) compared to *mdx* littermates (Figure 1D), and continued weight loss (Figure 1E). Mice that were given a mixture of powdered food and water in a dish maintained their weight for a longer time; however, all mice succumbed to premature death by 20 weeks of age.

Characterization of Skeletal Muscle from Dko Mice

mdx mice do not show any muscle pathology until 3 to 4 weeks after birth, when the onset of necrosis is first seen in the diaphragm muscle. The timing of the age of onset of muscular dystrophy in these mice has been hypothesized to correspond to the disappearance of utrophin from around the sarcolemma (Clerk et al., 1993). To determine the age of onset of muscular dystrophy in the dko mice, diaphragm muscles from 6-day-old and 2-week-old dko mice were examined and compared with diaphragm muscles from *mdx* littermates. Large areas of necrotic fibers and connective tissue with little evidence of regeneration were seen in the diaphragm of the 6-day-old dko but not in the age-matched *mdx* littermates (data not shown). Diaphragm muscles from 2-week-old dkos show these characteristics in addition to large numbers of centrally nucleated fibers, demonstrating that muscle fiber regeneration is now occurring (Figure 2, top).

Diaphragm muscles from 8-week dkos (Figure 3B) show the characteristic morphological abnormalities seen in *mdx* diaphragms (Figure 3A) with variation in muscle fiber diameter and staining intensity, centralized nuclei, and fibrosis. Ultrastructural analysis of 10-week dko diaphragms further illustrates severe muscle degeneration and fibrosis (data not shown). Although there is not as much connective tissue in dko diaphragms just prior to death as compared with diaphragms from 18-month-old *mdx* mice (Figure 3C) as assessed by light microscopy analysis, the lack of compensation by intercostal muscles may result in respiratory failure.

Central nuclei are present in fibers that have regenerated, and the percentage of centrally nucleated fibers is indicative of the amount of regeneration that has occurred in a muscle. The percentage of centrally nucleated fibers present in diaphragm muscles from 8-week-old dko mice is 39.5%, compared with 38.3% present in diaphragm muscles from age-matched *mdx* controls (Table 1A). These data suggest that the muscles from the dko mice possess the same history of regeneration as seen in *mdx* mice.

To assess sarcolemmal damage, diaphragm muscles from five dko mice that were still fairly mobile, one with

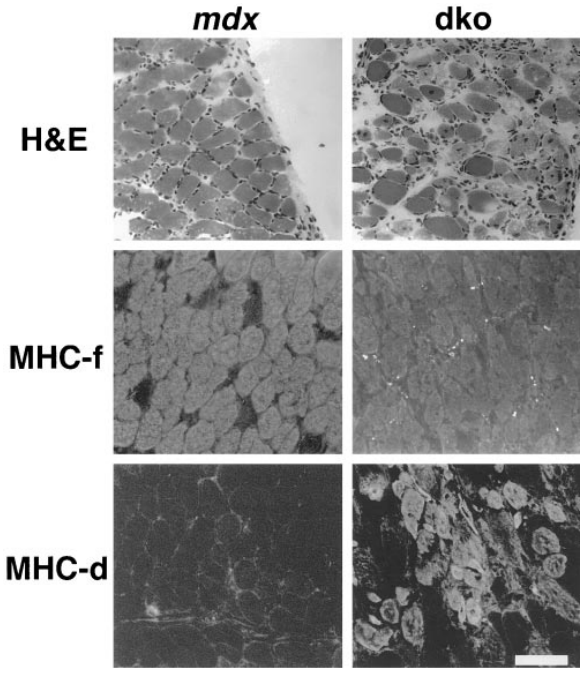

Figure 2. Dko Diaphragm Shows DMD-like Characteristics by Two Weeks of Age

H&E-stained diaphragm section from a 2-week-old dko mouse shows the onset of a dystrophic pathology (top right). This phenotype contrasts the normal diaphragm morphology seen in *mdx* littermate at the same age (top left). Immunohistochemistry with an antibody raised against myosin heavy chain "fast" isoform (MHC-f) shows expression in almost all (>99%) fibers from a 2-week-old dko diaphragm (middle right). In contrast, only ~90% of fibers in an age-matched *mdx* diaphragm muscle express this isoform with a characteristic scattered pattern of unstained fibers (middle left). "Developmental" myosin heavy chain (MHC-dev) is not expressed in 2-day-old *mdx* diaphragm (bottom left) but is present in small and large-caliber fibers in dko diaphragm muscles (bottom right). Bar = 90 μm.

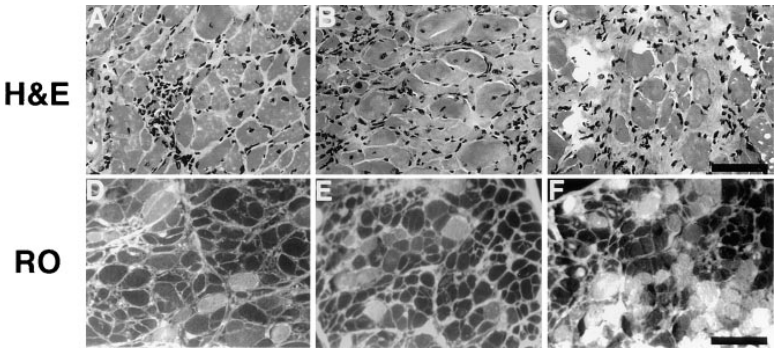

Figure 3. Diaphragm Muscles from Age-Matched *mdx* and Dko Mice Display a Similar Pathology

H&E-stained unfixed frozen diaphragm sections from 18-week-old *mdx* (A) and dko (B) mice show similar amounts of necrosis, fibrosis, and regeneration. Diaphragm muscles from 8-month-old *mdx* mice (C) contain a much higher proportion of collagen than do dko mice, suggesting that the fibrosis of the diaphragm muscle is not the primary cause of death in dko mice. Uptake of reactive orange by necrotic fibers in the diaphragm muscles of *mdx* (D) and dko (E) mice appears equivalent in the majority of sections analyzed. The diaphragm from a dko mouse that was assayed just prior to its natural death (F) shows a much higher proportion of necrotic fibers. It is unknown whether this observation is a primary or secondary effect of the physical state of the animal just prior to analysis. Bar = 62.5 μm.

severe weight loss and complete loss of mobility, and six *mdx* controls, all at 10 weeks of age, were immersed in a fluorescent, low molecular weight dye (reactive orange MW 631). This dye does not penetrate through intact membranes but stains the cytoplasm of fibers with compromised membrane integrity. The diaphragm muscles from the five moderately healthy dkos (Figure 3E) showed similar amounts of necrotic fibers to those seen in the diaphragms of their *mdx* littermates (Figure 3D). The severely affected dko had a much higher proportion of necrotic fibers (Figure 3F). It is unknown whether this higher rate of necrosis was a cause or a result of the physical state of this mouse. However, these observations suggest overall that membrane integrity is not different between dko and *mdx* mice.

Limb, axial, and heart muscles from adult littermates of all four genotypes (wild type, *mdx*, *utrn*$^{-/-}$, and dko) were examined by H&E staining. Utrophin-deficient tibialis anterior (TA) muscle appears morphologically normal (data not shown) until at least 1 year of age. In *mdx* TA muscle, there are irregularly shaped and sized muscle fibers, many with centralized nuclei and some lymphocyte infiltration (Figure 4). The dko TA muscle also shows extensive regeneration (central nuclei) and the presence of macrophages (Figure 4). In gastrocnemius and quadriceps muscles of dko and *mdx* mice (Figure 4), many eosinophilic and basophilic fibers are present. Some fibers seem to contain fat or appear to be replaced by adipose cells, as observed in advanced DMD biopsies (Dubowitz, 1978). Similar results were seen for extensor digitorum longus (EDL), soleus, and paraspinal muscles (data not shown). Histological analysis of dko and *mdx* hearts shows similar variability in the minimal amounts of necrosis and fibrosis (data not shown), and dko hearts did not appear to show any signs of a dilated cardiomyopathy. Overall, the skeletal and cardiac muscle morphology of the dko mice is not drastically worse than that of *mdx* mice.

It is observed that *mdx* mice undergo fiber hypertrophy (Figure 4), presumably to increase muscle mass to compensate for the loss of force-generating capacity due to dystrophin deficiency. To determine the capacity for hypertrophy of dko limb muscles, the masses of TA, EDL, and soleus muscles from each leg of four 10-week-old dko mice and four *mdx* littermates were determined

Table 1. Quantitative Analysis of Dko versus *mdx* Muscle

A. Centrally Nucleated Fibers in the Diaphragm		
	mdx	Dko
	38.3% (n = 1679)	39.5% (n = 2595)
B. Muscle Mass Relative to Total Body Mass		
	mdx	Dko
TA	.0053	.0045
EDL	.0010	.0012
Sol	.00077	.00073

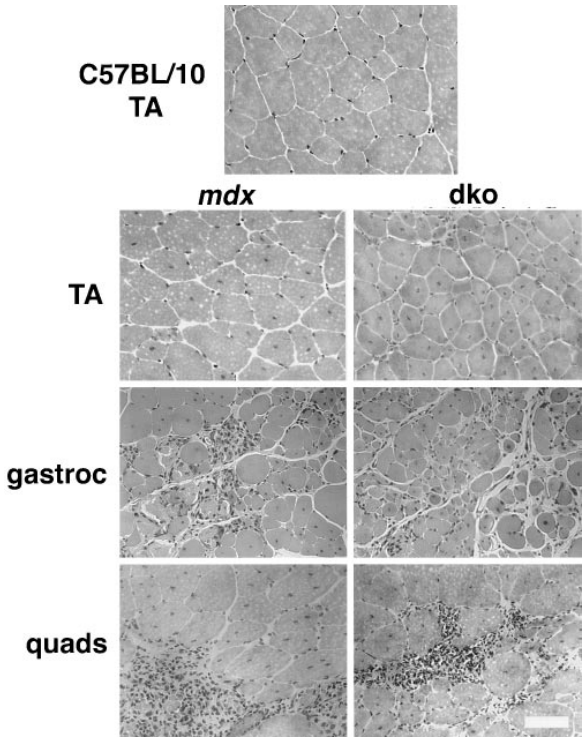

Figure 4. Hindlimb Muscles from Dko and *mdx* Mice Show a Similar Pathology

H&E-stained unfixed frozen sections of TA and quadriceps muscles and paraffin-embedded sections of gastrocnemius, from *mdx* and dko littermates at ~10 weeks of age, show variations in fiber size, necrosis, fibrosis, and centrally nucleated fibers. Bar = 120 μm.

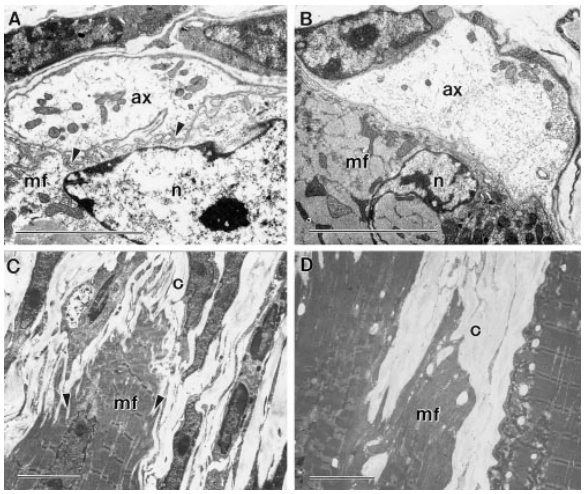

Figure 5. Ultrastructural Analysis of NMJs and MTJs

Typical NMJ morphology in the diaphragm (A and B) and MTJ morphology in the soleus muscle (C and D) of *mdx* (A and C) and dko (B and D) mice at 10 weeks. The junctional folds seen in the *mdx* (indicated by arrowheads) are notably absent in the dko mice. ax, axon; mf, muscle fiber; c, connective tissue; n, nucleus. Bar = 5 μm.

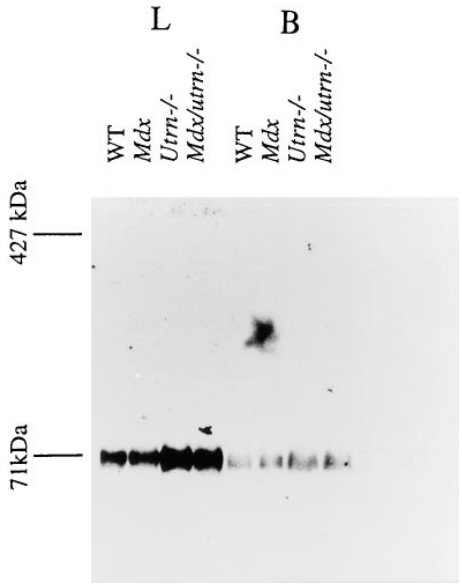

Figure 6. Dp71 Is Overexpressed in Lung and Brain in the Absence of Utrophin

Immunoblot of lung and brain total protein samples with a monoclonal antibody with specificity for the C terminus of dystrophin. The C-terminal Dp71 isoform of dystrophin is expressed in these nonmuscle tissues and appears to be upregulated in *utrn*$^{-/-}$ and dko samples.

and compared with the total body weights of the animals (Table 1B). No significant differences ($p < 0.05$) were detected between dko and *mdx* mice for any of these three muscle types. These data suggest that the capacity for hypertrophy seen in the *mdx* mouse is unaffected by the additional utrophin deficiency. However, it should be noted that body weights were significantly reduced in the dko mice compared with *mdx* littermates (see Figure 1E).

Ultrastructure of Neuromuscular and Myotendinous Junctions in Dko Mice

To assess the morphology of the pre- and postsynaptic regions of the NMJs in the absence of utrophin and dystrophin, diaphragm muscles from 10-week-old dko and *mdx* littermates were examined by transmission electron microscopy. At the NMJ in the diaphragm muscles of dko mice at 10 weeks, the nerve terminals of the axons appeared to be the same as those observed in *mdx* muscle. However, an examination of the postsynaptic motor endplate regions revealed a striking phenotypic abnormality with the virtual absence of folding at the postsynaptic membrane (Figure 5B). By contrast, the majority of *mdx* endplates displayed varying degrees of postsynaptic folding (Figure 5A), although approximately one-third show a similar morphology to that displayed by dko mice. None of the endplates examined were associated with obviously necrotic fibers. These data suggest a role for utrophin and dystrophin in the development or maintenance of junctional folds at the postsynaptic motor endplate.

The MTJs of normal mice are characterized by extensive finger-like projections of the sarcolemmal membrane. These folds serve to increase the surface area for the attachment of the muscle fiber to the connective tissue of the tendon and are thought to play an important role in the transmission of force between the muscle fiber and the tendon. A comparison of this region in the dko and *mdx* soleus revealed a marked reduction in membrane folding in the dko (Figure 5D) relative to the *mdx* (Figure 5C), suggesting that force transmission may be impaired in dko skeletal muscle.

Compensation by Dystrophin C-Terminal Isoforms Is Absent in Dko Skeletal Muscle

The strain of *mdx* mice used for interbreeding has normal expression of the four shorter C-terminal dystrophin isoforms (Dp71, Dp116, Dp140, and Dp260) (for review, see Blake et al., 1996). The specificity of expression of these different isoforms, as well as implication for involvement in cognitive and ocular defects, suggests a defined role for these dystrophin isoforms (Blake et al., 1996). The reduced neonatal survival rate due to poor maternal care of another *mdx* strain, *mdx3Cv*, which lacks all of the dystrophin locus transcripts, strengthens this suggestion (Cox et al., 1993). The absence of any aberrantly expressed C-terminal dystrophin isoforms in *mdx* and dko skeletal muscle was confirmed by Western analysis (data not shown). The fact that dko muscle, the only tissue where shorter transcripts are normally absent, shows severe phenotypic abnormalities suggests that these dystrophin C-terminal isoforms may be able to compensate for the absence of full-length utrophin and dystrophin in nonmuscle tissues. Consistent with this, there is some indication that Dp71 levels are increased in nonmuscle tissues such as lung and brain, both from *utrn*$^{-/-}$ and dko mutants (Figure 6).

DPC Localization to the NMJs Is Not Dependent on Dystrophin or Utrophin

Immunohistochemistry on sectioned soleus or quadriceps muscles from wild type, *mdx*, *utrn*$^{-/-}$, and dko was

performed using a panel of antibodies raised against DPC proteins. Sections were costained with α-bungarotoxin that binds to acetylcholine receptors (AChRs) and thereby labels NMJs. Antibodies raised against dystrophin-stained wild type and *utrn*$^{-/-}$ sarcolemma, with increased staining at the NMJ, presumably due to junctional folds that increase the amount of membrane able to accommodate dystrophin. Dystrophin was absent in *mdx* and dko muscle, except for rare revertant fibers (data not shown). Utrophin was localized exclusively to the NMJ in wild-type muscle, with additional weak sarcolemmal localization in *mdx* muscle, but was not present in *utrn*$^{-/-}$ or dko muscle (data not shown).

To assess the localization of members of the DPC, antibodies specific for several members of the complex were used to immunostain quadriceps muscle sections from wild-type, *mdx*, and dko mice. Members of the DPC are greatly reduced at the sarcolemma of muscle fibers of *mdx* mice compared with wild-type mice (Figure 7). Immunostaining with antibodies raised against β-dystroglycan (Figure 7) and α-sarcoglycan (data not shown) on dko and *mdx* quadriceps muscle sections shows similar localization at the NMJs and at low levels around the sarcolemma (Figure 7). In Western analysis, a reduction similar to that seen in *mdx* muscle was observed in muscle from the dko mice, and no reduction was observed in nonmuscle tissues (data not shown). Immunohistochemistry with antibodies raised against β2-syntrophin shows that it is localized normally at the NMJs of dko mice (Figure 7).

In *mdx* heart, α- and γ-sarcoglycan are only slightly reduced. There appear to be increased levels of utrophin in *mdx* heart, implying that utrophin may be responsible for these relatively normal levels of DPC proteins (Pons et al., 1994b). However, Western analysis indicates that levels of DPC proteins in dko heart are not reduced when compared to *mdx* heart, again indicating that utrophin may not be an alternative binding partner (data not shown).

Localization of Other Pre- and Postsynaptic Proteins Is Unaffected in Dko Mice

The abundance of the AChR shows an ∼40% decrease at the *utrn*$^{-/-}$ NMJs as shown by α-bungarotoxin labeling (Deconinck et al., 1997). Rapsyn, an NMJ-specific protein that colocalizes with AChRs and utrophin at the crests of the synaptic folds, (Apel et al., 1995) is localized normally in the dkos (Figure 7). The NMJ-specific marker acetylcholine esterase appears more scattered, which may reflect not fully clustered AChRs and thus immature muscle (data not shown). MuSK, a postsynaptic protein that serves as the agrin receptor, also retains its localization to the NMJs of the dko mice (data not shown) (Valenzuela et al., 1995; DeChiara et al., 1996). The persistence of AChRs, rapsyn, and MuSK indicates that utrophin is not required for the normal clustering of any of the members of the AChR complex.

Coexpression of Myosin Heavy Chain Isoforms in Dko Skeletal Muscle

In general, glycolytic myofibers express "fast" isoforms of MHC. Fast fibers can be further broken down into at least three subclasses (Schiaffino et al., 1989; Schiaffino and Reggiani, 1994). Oxidative fibers normally express a different "slow" isoform of MHC. The ratio of fast to slow fibers differs between muscles and between species, although a combination of the two basic classes appears to be ubiquitous (Yellin, 1967; Jolesz and Sreter, 1981; Cho et al., 1993). Sections of diaphragm muscles from 2-, 8-, and 10-week-old wild-type, *mdx*, *utrn*$^{-/-}$, and dko mice were analyzed immunohistochemically with antibodies specific for fast, slow, or developmental MHC isoforms. Antibodies raised against the "fast" MHC isoform stained about 90% of fibers in diaphragm muscle from wild-type mice and a slightly higher percentage of fibers in *mdx* diaphragm muscle. However, >99% of fibers in the diaphragms of the dko mice stained with fast MHC, suggesting a difference in the proportion of oxidative muscle in these mice. Antibodies against the developmental MHC isoform stained only small-caliber, newly regenerated fibers in *mdx* diaphragm muscle. However, large-caliber, noncentrally nucleated "mature" fibers in dko diaphragms were detected with this antibody. This pattern of MHC isoform expression was seen at least as early as 2 weeks of age (Figure 2). Similar coexpression of MHC isoforms was also seen in soleus muscles (data not shown). Elevated levels of the developmental MHC isoform in nonregenerating fibers and coexpression of developmental, slow, and/or fast MHC isoforms in the same fibers suggest a role for utrophin and dystrophin in muscle development or MHC-isoform expression.

Discussion

The data presented in this paper show that mice deficient in both dystrophin and utrophin show a severe progressive muscle-wasting disorder with early onset and death within 20 weeks. These results demonstrate the synergy of these two proteins and also provide evidence that the double mutant will be a valuable model for the detailed study of the pathogenesis of DMD. Grady et al. (1997b) show similar results (see accompanying paper [this issue of *Cell*]).

DMD patients are gravely affected by absence of dystrophin, unlike the *mdx* mouse, which has no clinical features and a relatively normal life span. It is possible that the rate of progression of the myopathy due to the lack of dystrophin in mice and humans is similar and that the two-year life span of a mouse is not long enough for the manifestation of the underlying muscle pathology. It is believed that *mdx* mice compensate for lack of dystrophin by increased muscle regeneration and upregulation of other proteins, such as muscle transcription factors, e.g., MyoD and structurally related proteins such as utrophin (Matsumura et al., 1992). In view of the embryonic expression pattern of utrophin and its exclusive localization at the NMJ and other cell–cell communication sites, *utrn*$^{-/-}$ mice display a surprisingly mild phenotype (Deconinck et al., 1997; Grady et al., 1997a). The generation of a novel mouse mutant with a severe dystrophic phenotype, premature death, and many cellular characteristics of DMD through the interbreeding of *mdx* mice and *utrn*$^{-/-}$ mice suggests that

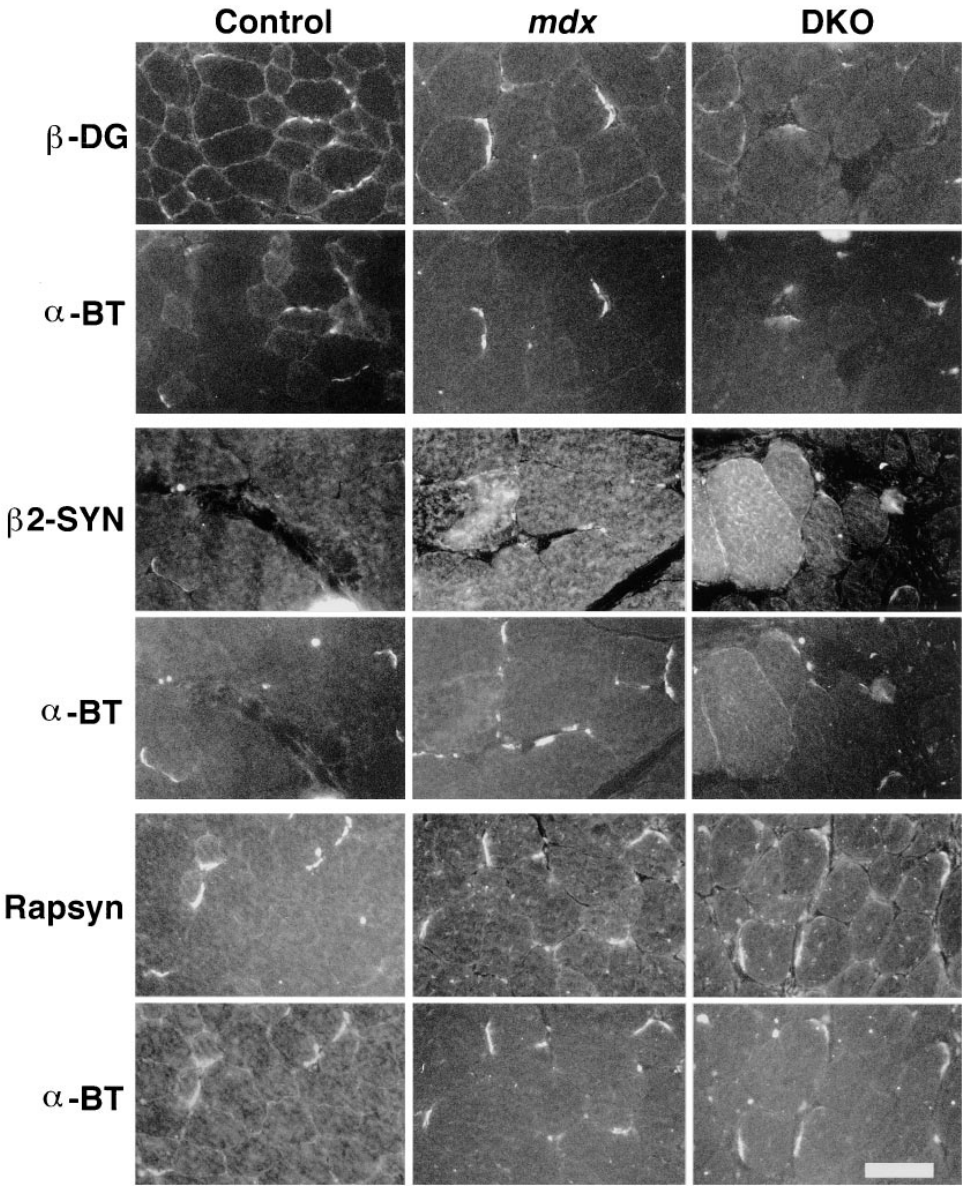

Figure 7. Members of the Dystrophin-Associated and AChR Complexes Remain Localized at the NMJ in the Absence of Utrophin and Dystrophin

Immunofluorescence analysis of C57 wild-type, *mdx*, and dko quadriceps sections with antibodies raised against β-dystroglycan, β2-syntrophin, and rapsyn show localization of all proteins at the NMJs in dko mice. Sections were costained with BODIPY-conjugated α-bungarotoxin (BT) that binds to AChRs.

the mild phenotypes seen in the single mutants may be due to functional compensation between utrophin and dystrophin.

The dko mice display marked myopathy, leading to weight loss and breathing difficulties, resulting in premature death. The primary cause of death of the dko mice is most likely respiratory failure, but we are unable to rule out contributions from such factors as cardiac complications or the inability to eat and drink properly due to weak tongue muscles. Histopathological analysis of muscle sections shows many of the characteristic features also described in DMD biopsies and to a lesser extent in the *mdx* mouse, including variation in muscle fiber size, connective tissue proliferation, extensive regeneration (most fibers have central nuclei), replacement by adipose cells, presence of necrotic fibers, and invasion by macrophages. The paraspinal and gastrocnemius muscles are the most severely affected muscles, both in *mdx* and dko mouse mutants and in DMD patients. Many of the clinical features such as waddling gait, arched spine, and premature death displayed by the double mutants are similar to those described in DMD patients. In contrast, *mdx* mice, which show a more severe muscle pathology in older age than the dkos do at the time of death, do not display these overt abnormalities at ages of at least one year.

There are several mechanisms that may contribute to the phenotype of the dko mice. In view of the NMJ-specific localization of utrophin, a defect in muscle innervation may underlie some of the dystrophic symptoms. AChE appears slightly less clustered around some fibers in dko mice (data not shown), an initial indication that there may be a developmental delay, as immature muscle is typified by unclustered synaptic proteins (Vincent et al., 1997). However, our data suggest that postsynaptic proteins such as AChRs, rapsyn, and MuSK are localized normally.

A reduction in the degree of folding at the postsynaptic membrane of the neuromuscular junction has previously been noted in both *mdx* (Torres and Duchen, 1987; Nagel et al., 1990; Lyons and Slater, 1991) and *utrn*$^{-/-}$ mice (Deconinck et al., 1997; Grady et al., 1997a). Moreover, approximately half of DMD endplates show ultrastructural abnormalities consisting of focal degeneration of the postsynaptic junctional folds, simplification of the postsynaptic region, and/or widening of the synaptic cleft (Jerusalem et al., 1974). In normal muscle, dystrophin is concentrated at the base of the postsynaptic folds, where there is a high density of voltage-gated sodium channels (Flucher and Daniels, 1989; Sealock et al., 1991; Bewick et al., 1992). However, its role in this location with respect to the folds remains unclear, as ultrastructural alterations at the *mdx* endplate are thought to be a consequence of the effects of fiber degeneration and regeneration rather than directly attributable to the absence of dystrophin (Lyons and Slater, 1991). Utrophin localizes to the crests of the postsynaptic folds, and its absence in *utrn*$^{-/-}$ mice has been shown to be associated with a reduction in postsynaptic folding and the number of AChRs (Deconinck et al., 1997). Interestingly, the absence of both utrophin and dystrophin in dko mice fails to alter the general localization of other NMJ-specific proteins such as rapsyn and MuSK. However, the spatial organization and segregation of sodium channels and AChRs will be affected by the absence of folds at the postsynaptic cleft. These observations taken together with those of *mdx* and *utrn*$^{-/-}$ mice tend to imply a role for utrophin and dystrophin in the development and/or stabilization of postsynaptic folds that may be severely compromised either directly by the absence of dystrophin at the base of the folds or indirectly by the successive rounds of muscle fiber regeneration characteristic of dystrophin-deficient muscle.

The functional consequences of postsynaptic fold reduction at the NMJ of the *mdx* mouse seem to be minimal, since neither the miniature endplate potential frequency, quantal content of endplate potential, amplitude, and time course of miniature endplate currents or the number of AChRs appear to be abnormal (Nagel et al., 1990; Lyons and Slater, 1991). In *utrn*$^{-/-}$ mice, a reduction in the extent of postsynaptic folding leads to a reduction in the number of AChRs but only minimal electrophysiological alterations (Deconinck et al., 1997). Thus, *mdx* and single-knockout *utrn*$^{-/-}$ mice show only subtle ultrastructural alterations at the endplate, and neuromuscular transmission does not appear to be greatly impaired. In the case of the dko mice, the almost complete absence of postsynaptic folding in the dko diaphragm must cause gross disruption in the spatial organization of receptors and ion channels. Under these conditions, defects in neuromuscular transmission might be expected to be particularly deleterious, especially in a muscle such as the diaphragm, which is subjected to continual stimulation throughout life. However, miniature endplate potentials do not appear different from those observed in *utrn*$^{-/-}$ mice (T. Wang and A. Vincent, personal communication). Therefore, the significance of the reduction of the postsynaptic folding remains unknown.

A reduction in folding at the MTJ has previously been noted in *mdx* mice, although this defect appears to have no detectable effects on the stress, strain, or energy absorbed in this region. *mdx* muscle, if lengthened to the point of rupture, fails at the same stress level as identically loaded control muscle (Law et al., 1995). However, the reduction in folding evident at the dko MTJ might be expected to increase markedly the forces placed on individual contact areas between the fiber membrane and connective tissue matrix thus leading to membrane damage in this region. Since muscle grows by the addition of sarcomeres in this region, such defects may also profoundly influence muscle growth.

Since the levels of the DPC are greatly reduced around the sarcolemma in the absence of dystrophin, and utrophin has been shown to be capable of interacting with the DPC in utrophin/*mdx* transgenic mice (Tinsley et al., 1996), we predicted that the members of the DPC would be greatly reduced or completely absent at the NMJ in the absence of dystrophin and utrophin. However, all DPC proteins analyzed are retained at the NMJ in dko skeletal muscles. β-2 syntrophin, which is normally localized to the NMJ (Peters et al., 1994) and was hypothesized to bind to the C-terminal region of utrophin, is also localized normally in the absence of dystrophin and utrophin. These data suggest that the localization of these proteins at the NMJ is not dependent upon interactions with utrophin, even though DPC localization at the rest of the sarcolemma is dependent upon interaction with dystrophin. Therefore, either there is some inherent aspect of the membrane itself at the NMJ that is responsible for the maintenance of the DPC, or there is an unspecified protein present at the NMJ that is responsible for the stability of this protein complex. These data suggest that dystrophin and utrophin have other functions in addition to those involving the DPC and have major implications regarding current models depicting the organization of the DPC complex at the NMJ. However, the continued localization of these proteins at the NMJ represents one more similarity between dko mice and DMD patients.

The most dramatic cellular differences between *mdx* and dko muscles are skewed ratios of fast-to-slow-twitch muscle fibers and the preponderance of fibers that coexpress multiple MHC isoforms. Developmental isoforms of MHC in large-caliber fibers are only observed in dko muscle, suggesting a problem in muscle maturation. The lack of slow MHC or oxidative fibers in the diaphragm muscle may account for the morbidity observed in the dko mice. The reliance on glycolytic muscle fibers in the diaphragm for typical slow-twitch activities such as breathing may tax the energy output

mechanisms of the muscle and could lead to respiratory failure (Prakash et al., 1996). These observations of MHC isoform expression correlate well with those seen in a study of nine DMD patients (Marini et al., 1991) and therefore define another similarity to DMD that is not seen to a significant extent in *mdx* mice.

The data presented here illustrate that, in addition to the previously described structural role at the NMJ (Deconinck et al., 1997; Grady et al., 1997a), utrophin may also have an important function in dystrophin-deficient muscle. Such a proposal does not appear to be consistent with the mild phenotype described for *utrn*$^{-/-}$ mice. However, the lack of myopathy in the utrophin-knockout mice may be the result of the continued localization of dystrophin at the NMJ, possibly stabilizing the utrophin-deficient junctional folds. A consideration of the phenotypes of each single-knockout mouse compared with the phenotype of mice deficient for both utrophin and dystrophin suggests that these two proteins play roles in complementing developmental or functional pathways. The loss of both proteins results in far greater consequences than simply the combination of the two independent phenotypes. Overexpression of either protein may fully compensate for the loss of the other, as suggested by the recent report describing the prevention of the dystrophic phenotype of *mdx* mice with a utrophin transgene (Tinsley et al., 1996).

Further analysis is being carried out to investigate the function of utrophin in cardiac muscle and other tissues where utrophin is highly expressed. Although we do not observe any dilated cardiomyopathies in these mice, there could certainly be milder cardiac abnormalities for which we cannot account. The relative contributions of each type of striated muscle to the primary cause of death in these mice must await the generation of dko mice expressing utrophin transgenes in a variety of patterns in limb muscles, diaphragm, and heart.

Finally, a variable neurogenic component may exist in the pathology of DMD, particularly in relation to periods of ongoing degeneration. In addition, dystrophin and utrophin are components of the postsynaptic apparatus in many CNS neurons, particularly the cerebral cortex. The dko mice may thus serve as a model not only to study potential therapies for DMD and the basic cell biology of the NMJ but also to provide clear insights into subtle neurogenic components in the pathology of the muscular dystrophies as a whole.

Experimental Procedures

Breeding Schemes

Mice deficient in both dystrophin and utrophin (double knockouts) were derived by a breeding program as follows: female C57Bl/10 *mdx* mice (deficient in dystrophin) were mated with male utrophin-null mice (*utrn*$^{-/-}$) (Deconinck et al., 1997), resulting in an F1 generation heterozygous for utrophin and either heterozygous for the *mdx* mutation (females) or hemizygous for the *mdx* mutation (males). This F1 generation was used to produce dko mice in three ways:

(A) Male F1 (*utrn*$^{+/-}$, *mdx*) $\times$ female *mdx* (*utrn*$^{+/+}$, *mdx/mdx*) gave an F2 generation all *mdx* and either wild type or heterozygous at the utrophin locus. Male and female F2 mice heterozygous for the utrophin knockout were mated and the progeny were all *mdx*, of which 25% were *utrn*$^{-/-}$ (dkos). *utrn*$^{+/+}$, *mdx/mdx* littermates resulting from this mating scheme were used as *mdx* control littermates in all dko analyses.

(B) Female F1 (*utrn*$^{+/-}$, *mdx*$^{+/-}$) $\times$ male utrophin knockouts (*utrn*$^{-/-}$) produced F2s where 25% of the males were dkos.

(C) Male F1 (*utrn*$^{+/-}$, *mdx*) $\times$ female F1 (*utrn*$^{+/-}$, *mdx*$^{+/-}$) produced Mendelian ratios of utrophin and dystrophin. 12.5% of the progeny were dkos.

Genotyping

DNA from tail biopsies was analyzed by ARMS assay PCR as previously described to screen for the *mdx* allele (Amalfitano and Chamberlain, 1996). PCR analysis to determine utrophin-knockout status used a forward primer complementary to exon 7 of mouse utrophin (5′ GTG AAG GAT GTC ATG AAA G 3′) and reverse primers complementary to either intron 7 (5′ TGA AGT CCG AAA GAG ATA CC 3′) or to the PGK promoter located within the Neo-knockout cassette (5′ ACG AGA CTA GTG AGA CGT GC 3′). Reactions were carried out on genomic DNA for 35 cycles under the following conditions: 94°C, 30 s; 57°C, 30 s; 72°C, 25 s.

Histological Analysis

Mice were sacrificed and tissues excised, embedded in Cryo-M-Bed (Bright, Huntingdon, Cambs, England), frozen in liquid nitrogen-cooled isopentane. Frozen sections (8 μm) of these quadriceps, soleus, and diaphragm samples were cut on a cryostat. TA and gastrocnemius samples were fixed in paraformaldehyde and embedded in paraffin. All sections were stained with hematoxylin and eosin (H&E) as standard.

Western Analysis

Tissues were homogenized in gel loading buffer (75 mM Tris-HCl [pH 6.8], 3.8% SDS, 4 M urea, and 20% glycerol) and the total protein content assessed (Bio-Rad DC Assay kit). Following addition of 5% β-mercaptoethanol and 0.001% bromophenol blue, 100 μg of each extract was separated on an SDS-polyacrylamide gel (8% for dystrophin and utrophin; 12% for β-dystroglycan) and electroblotted onto a nitrocellulose membrane. The membranes were then incubated with antibodies to utrophin (MANCHO7), or dystrophin (MANDYS1 and MANDRA1, all used at 1/100; kind gifts of Dr. G. E. Morris). Bound primary antibodies were detected by horseradish peroxidase-conjugated secondary antibodies followed by chemiluminescence (Boehringer).

Immunofluorescence Analysis

All immunolabeling was done on 8 μm thick unfixed sections of muscle frozen in isopentane cooled in liquid nitrogen. Sections were preincubated with 1% gelatin in potassium-phosphate-buffered saline (KPBS) for 30 min at room temperature. Antibodies were applied in KPBS plus 0.2% gelatin plus 1% normal goat serum for 2 hr at room temperature. Primary antibodies against the following proteins were used: utrophin, dystrophin (G3 [1/25] and P6 [1/800], polyclonals, kind gift of Dr. C. A. Sewry, London, UK), β-dystroglycan, α-sarcoglycan (polyclonals, kind gift of Dr. K. P. Campbell, Iowa), rapsyn, laminin (polyclonals raised by Dr. A. Vincent against recombinant proteins, kindly provided by Dr. J. R. Sanes, St. Louis), MuSK (polyclonal, used at 1/100, kind gift of Dr. S. Burden), fast and slow MHC isoforms (mouse monoclonals, Novacostra, Newcastle-upon-Tyne, UK), and developmental myosin (mouse monoclonal, kind gift of L. V. B. Anderson).

Immunoreactivity was visualized using secondary antibodies conjugated with FITC (Sigma). Sections were costained with BODIPY-α-BgTx (0.6×10^{-6} M, Molecular Probes) to identify NMJs. Labeled sections were mounted in Vectashield (Vector Laboratories) and viewed using a Leica DMRBE microscope. Sections incubated in dilutent without primary antibody served as controls for nonspecific binding of secondary antibodies.

Reactive Orange

Complete diaphragm muscles from *mdx* and dko mice were removed and soaked for 1 hr in 0.2% reactive orange (Sigma) in F10 tissue culture media (Sigma). Diaphragms were then rinsed briefly in F10 media, cut into pieces, embedded in Cryo-M-Bed (Bright, Huntingdon, Cambs, England), and frozen in liquid nitrogen-cooled isopentane. Sections (8 μm) were cut on a cryostat and visualized through an FITC filter using a Leica DMRBE microscope.

Ultrastructural Analysis

Excised muscles were fixed in 3% glutaraldehyde and 4% formaldehyde in 0.1 M PIPES buffer at pH 7.2 for 1 hr, postfixed in 1% osmium 0.1 M PIPES for 1 hr, and embedded in TAAB (TAAB Laboratories, Aldermaston, UK) resin. Gold/Silver (90 nm) sections were cut using a Cambridge Huxley MKII Ultramicrotome, stained with alcoholic uranyl acetate and lead stain, and viewed using a Zeiss EM109.

Acknowledgments

We wish to thank Anton Page for invaluable assistance with electron microscopy and preparation of the final manuscript, Derek Blake for helpful discussions, and Jeffrey Trickett for help with genotyping. We thank the Muscular Dystrophy Group of Great Britain and Northern Ireland, the Muscular Dystrophy Association USA, the Burroughs Wellcome Fund, the Medical Research Council, the Association Contre les Myopathies, and the EC Biotechnology program for funding this work.

Received April 15, 1997; revised June 27, 1997.

References

Amalfitano, A., and Chamberlain, J.S. (1996). The mdx-amplification-resistant mutation system assay, a simple and rapid polymerase chain reaction-based detection of the *mdx* allele. Muscle Nerve *19*, 1549–1553.

Apel, E.D., Roberds, S.L., Campbell, K.P., and Merlie, J.P. (1995). Rapsyn may function as a link between the acetylcholine receptor and the agrin-binding dystrophin-associated glycoprotein complex. Neuron *15*, 115–126.

Bewick, G.S., Nicholson, L.V., Young, C., O'Donnell, E., and Slater, C.R. (1992). Different distributions of dystrophin and related proteins at nerve-muscle junctions. Neuroreport *3*, 857–860.

Blake, D.J., Tinsley, J.M., and Davies, K.E. (1996). Utrophin: a structural and functional comparison to dystrophin. Brain Pathol. *6*, 37–47.

Bulfield, G., Siller, W.G., Wight, P.A., and Moore, K.J. (1984). X chromosome-linked muscular dystrophy (mdx) in the mouse. Proc. Natl. Acad. Sci. USA *81*, 1189–1192.

Campbell, K.P. (1995). Three muscular dystrophies: loss of cytoskeleton-extracellular matrix linkage. Cell *80*, 675–679.

Cho, M., Webster, S.G., and Blau, H.M. (1993). Evidence for myoblast-extrinsic regulation of slow myosin heavy chain expression during muscle fiber formation in embryonic development. J. Cell Biol. *121*, 795–810.

Clerk, A., Morris, G.E., Dubowitz, V., Davies, K.E., and Sewry, C.A. (1993). Dystrophin-related protein, utrophin, in normal and dystrophic human fetal skeletal muscle. Histochemical J. *25*, 554–561.

Cox, G.A., Phelps, S.F., Chapman, V.M., and Chamberlain, J.S. (1993). New mdx mutation disrupts expression of muscle and non-muscle isoforms of dystrophin. Nat. Genet. *4*, 87–93.

Cullen, M.J., and Jaros, E. (1988). Ultrastructure of the skeletal muscle in the X chromosome-linked dystrophic (mdx) mouse. Comparison with Duchenne muscular dystrophy. Acta Neuropathol. Berl. *77*, 69–81.

DeChiara, T.M., Bowen, D.C., Valenzuela, D.M., Simmons, M.V., Poueymirou, W.T., Thomas, S., Kinetz, E., Compton, D.L., Rojas, E., Park, J.S., Smith, C., DiStefano, P.S., Glass, D.J., Burden, S.J., and Yancopoulos, G.D. (1996). The receptor tyrosine kinase MuSK is required for neuromuscular junction formation in vivo. Cell *85*, 501–512.

Deconinck, A.E., Potter, A.C., Tinsley, J.M., Wood, S.J., Vater, R., Young, C., Metzinger, L., Vincent, A., Slater, C.R., and Davies, K.E. (1997). Postsynaptic abnormalities at the neuromuscular junctions of utrophin-deficient mice. J. Cell Biol. *136*, 883–894.

Dubowitz, V. (1978). Muscle Disorders in Childhood, 2nd Ed. (London: W.B. Saunders Company Ltd.).

Emery, A.E.H. (1993). Duchenne Muscular Dystrophy, 2nd Ed. (Oxford: Oxford University Press).

Flucher, B.E., and Daniels, M.P. (1989). Distribution of Na^+ channels and ankyrin in neuromuscular junctions is complementary to that of acetylcholine receptors and the 43 kDa protein. Neuron *3*, 163–175.

Grady, R.M., Merlie, J.P., and Sanes, J.R. (1997a). Subtle neuromuscular defects in utrophin-deficient mice. J. Cell Biol. *136*, 871–882.

Grady, R.M., Teng, H., Nichol, M.C., Cunningham, J.C., Wilkinson, R.S., and Sanes, J.R. (1997b). Skeletal and cardiac myopathies in mice lacking utrophin and dystrophin: a model for Duchenne muscular dystrophy. Cell, this issue, *90*, 729–738.

Helliwell, T.R., Man, N.T., Morris, G.E., and Davies, K.E. (1992). The dystrophin-related protein, utrophin, is expressed on the sarcolemma of regenerating human skeletal muscle fibers in dystrophies and inflammatory myopathies. Neuromuscul. Disord. *2*, 177–184.

Jerusalem, F., Engel, A.G., and Gomez, M.R. (1974). Duchenne dystrophy. II. Morphometric study of motor end-plate fine structure. Brain *97*, 123–130.

Jolesz, F., and Sreter, F.A. (1981). Development, innervation, and activity-pattern induced changes in skeletal muscle. Annu. Rev. Physiol. *43*, 531–552.

Karpati, G., Carpenter, S., Morris, G.E., Davies, K.E., Guerin, C., and Holland, P. (1993). Localization and quantitation of the chromosome 6-encoded dystrophin-related protein in normal and pathological human muscle. J. Neuropathol. Exp. Neurol. *52*, 119–128.

Law, D.J., Allen, D.L., and Tidball, J.G. (1994). Talin, vinculin and DRP (utrophin) concentrations are increased at the *mdx* myotendinous junctions following onset of necrosis. J. Cell Sci. *107*, 1477–1483.

Law, D.J., Caputo, A., and Tidball, J.G. (1995). Site and mechanics of failure in normal and dystrophin-deficient skeletal muscle. Muscle Nerve *18*, 216–223.

Lyons, P.R., and Slater, C.R. (1991). Structure and function of the neuromuscular junction in young adult mdx mice. J. Neurocytol. *20*, 969–981.

Marini, J.F., Pons, F., Leger, J., Loffreda, N., Anoal, M., Chevallay, M., Fardeau, M., and Leger, J.J. (1991). Expression of myosin heavy chain isoforms in Duchenne muscular dystrophy patients and carriers. Neuromuscul. Disord. *1*, 397–409.

Matsumura, K., Ervasti, J.M., Ohlendieck, K., Kahl, S.D., and Campbell, K.P. (1992). Association of dystrophin-related protein with dystrophin-associated proteins in mdx mouse muscle. Nature *360*, 588–91.

Megeney, L.A., Kablar, B., Garrett, K., Anderson, J.E., and Rudnicki, M.A. (1996). MyoD is required for myogenic stem cell function in adult skeletal muscle. Genes Dev. *10*, 1173–1183.

Nagel, A., Lehmann, H.F., and Engel, A.G. (1990). Neuromuscular transmission in the mdx mouse. Muscle Nerve *13*, 742–749.

Ozawa, E., Yoshida, M., Suzuki, A., Mizuno, Y., Hagiwara, Y., and Noguchi, S. (1995). Dystrophin-associated proteins in muscular dystrophy. Hum. Mol. Genet. *4*, 1711–1716.

Peters, M.F., Kramarcy, N.R., Sealock, R., and Froehner, S.C. (1994). Beta 2-Syntrophin: localization at the neuromuscular junction in skeletal muscle. Neuroreport *5*, 1577–1580.

Pons, F., Robert, A., Fabbrizio, E., Hugon, G., Califano, J.C., Fehrentz, J.A., Martinez, J., and Mornet, D. (1994a). Utrophin localization in normal and dystrophin-deficient heart. Circulation *90*, 369–374.

Pons, F., Robert, A., Marini, J.F., and Leger, J.J. (1994b). Does utrophin expression in muscles of mdx mice during postnatal development functionally compensate for dystrophin deficiency. J. Neurol. Sci. *122*, 162–170.

Prakash, Y.S., Miller, S.M., Huang, M., and Sieck, G.C. (1996). Morphology of diaphragm neuromuscular junctions on different fiber types. J. Neurocytol. *25*, 88–100.

Schiaffino, S., and Reggiani, C. (1994). Myosin isoforms in mammalian skeletal muscle. J. Appl. Physiol. *77*, 493–501.

Schiaffino, S., Gorza, L., Sartore, S., Saggin, L., Ausoni, S., Vianello, M., Gundersen, K., and Lomo, T. (1989). Three myosin heavy chain isoforms in type 2 skeletal muscle fibers. J. Muscle Res. Cell Motil. *10*, 197–205.

Sealock, R., Butler, M.H., Kramarcy, N.R., Gao, K.X., Murnane, A.A., Douville, K., and Froehner, S.C. (1991). Localization of dystrophin

relative to acetylcholine receptor domains in electric tissue and adult and cultured skeletal muscle. J. Cell Biol. *113*, 1133–1144.

Sewry, C.A., Matsumura, K., Campbell, K.P., and Dubowitz, V. (1994). Expression of dystrophin-associated glycoproteins and utrophin in carriers of Duchenne muscular dystrophy. Neuromuscul. Disord. *4*, 401–409.

Sicinski, P., Geng, Y., Ryder, C.A., Barnard, E.A., Darlison, M.G., and Barnard, P.J. (1989). The molecular basis of muscular dystrophy in the mdx mouse: a point mutation. Science *244*, 1578–1580.

Tinsley, J.M., Blake, D.J., Zuellig, R.A., and Davies, K.E. (1994). Increasing complexity of the dystrophin-associated protein complex. Proc. Natl. Acad. Sci. USA *91*, 8307–8313.

Tinsley, J.M., Potter, A.C., Phelps, S.R., Fisher, R., Trickett, J.I., and Davies, K.E. (1996). Amelioration of the dystrophic phenotype of *mdx* mice using a truncated utrophin transgene. Nature *384*, 349–352.

Torres, L.F., and Duchen, L.W. (1987). The mutant mdx: inherited myopathy in the mouse. Morphological studies of nerves, muscles and end-plates. Brain *110*, 269–299.

Valenzuela, D.M., Stitt, T.N., DiStefano, P.S., Rojas, E., Mattsson, K., Compton, D.L., Nunez, L., Park, J.S., Stark, J.L., Gies, D.R., et al. (1995). Receptor tyrosine kinase specific for the skeletal muscle linkage: expression in embryonic muscle, at the neuromuscular junction, and after injury. Neuron *15*, 573–584.

Vincent, A., Newland, C., Croxen, R., and Beeson, D. (1997). Genes at the junction-candidates for congenital myasthenic syndromes. Trends Neurosci. *20*, 15–22.

Winder, S.J., Hemmings, L., Maciver, S.K., Bolton, S.J., Tinsley, J.M., Davies, K.E., Critchley, D.R., and Kendrick, J.J. (1995). Utrophin actin binding domain: analysis of actin binding and cellular targeting. J. Cell Sci. *108*, 63–71.

Yellin, H. (1967). Neural regulation of enzymes in muscle fibers of red and white muscle. Exp. Neurol. *19*, 92–103.